American Mineralogist, Volume 68, pages 687–698, 1983

Crystallization kinetics in the system $CaMgSi_2O_6$–$CaAl_2Si_2O_8$: the delay in nucleation of diopside and anorthite

AKIRA TSUCHIYAMA[1]

Geological Institute, University of Tokyo
Hongo, Tokyo 113, Japan

Abstract

Dynamic crystallization experiments on three different compositions in the system $CaMgSi_2O_6$–$CaAl_2Si_2O_8$ have been made in detail using the Pt-wire loop method. The nucleation of diopside and anorthite is always delayed under supercooled conditions. The delay in nucleation decreases with increasing degree of supercooling or increasing cooling rate. With further increase in the degree of supercooling or the cooling rate, the delay in anorthite nucleation increases. The incubation time for nucleation cannot be determined accurately because the nucleation takes place at random in some region of temperature–time space. For a given degree of supercooling, the region of random nucleation of diopside is wider than that of anorthite. Interpretations using nucleation theory indicate that steady-state nucleation occurs for diopside and transient nucleation for anorthite. The steady-state nucleation of diopside is verified by additional experiments to examine the nucleation probability of diopside. The delay in diopside nucleation and the region of the random nucleation decrease in experiments using Pt–Au capsules, in which heterogeneous nucleation takes place extensively. The effect of heterogeneous nucleation is also consistent with nucleation theory. The delay in anorthite nucleation was also investigated as a function of initial superheat and its duration for a given degree of supercooling. The delay increases with increasing initial superheat and its duration but becomes constant for an initial superheat greater than about 40°C and for a duration longer than about 45 min. These results can be explained by taking into account the equilibrium size distribution of crystal embryos in the liquid. Some implications of the experimental results for igneous petrology, such as estimation of cooling rate of magmas, effect of superheating or supercooling on the textures of igneous rocks and relative ease of mineral nucleation in magmas are also discussed.

Introduction

Many dynamic crystallization experiments have been carried out to produce textures of igneous rocks and to estimate conditions of crystallization of magmas (*e.g.*, Lofgren *et al.*, 1974; Donaldson *et al.*, 1975; Usselman *et al.*, 1975; Walker *et al.*, 1976; Lofgren, 1977; Grove and Bence, 1977; Grove, 1978; Lofgren, 1980). Many experimental studies of the morphology and compositions of minerals and measurements of the rates of nucleation and crystal growth have been also carried out in various systems (*e.g.*, Lofgren, 1974a,b; Kirkpatrick, 1974; Kirkpatrick *et al.*, 1976, 1981; Lofgren and Gooley, 1977; Fenn, 1977; Swanson, 1977).

In the present study, dynamic crystallization experiments were carried out in a simple system in order to understand the detailed kinetics of the crystallization processes. The system $CaMgSi_2O_6$–$CaAl_2Si_2O_8$ was chosen for the present experiments because it is one of the simplest yet most fundamental systems to simulate natural basic magmas. This paper deals with the nucleation kinetics. The development of textures, the compositional change of the liquid, and development of zoning of Al in diopside and Mg in anorthite will be discussed in future papers.

It has been found by various dynamic crystallization experiments that many silicate liquids can be supercooled to subliquidus conditions without nucleation of any crystalline phases (Gibb, 1974; Walker *et al.*, 1976; Grove, 1978; Grove and Bence, 1979; Donaldson, 1979; Gamble and Taylor, 1980; Grove and Beaty, 1981). It is known that the delay in nucleation plays a significant role in the development of textures (Lofgren, 1980). Gibb (1974) studied the delay in nucleation of plagioclase from a Columbia river basalt and found that the delay in plagioclase nucleation is dependent on the degree of supercooling, ΔT. With a systematic study of the delay of olivine

[1] Present address: NASA Johnson Space Center SN4, Houston, Texas 77058, U.S.A.

0003–004X/83/0708–0687$02.00

nucleation from basaltic melts, Donaldson (1979) found that the incubation time was dependent on cooling rate, initial superheat and composition of the liquid as well as on ΔT, and explained his results in terms of nucleation theory. The delay is also expected to depend on the duration of the initial superheat (Kirkpatrick, 1981), but there are no systematic data on this effect. In addition, heterogeneous nucleation is expected to affect the delay in nucleation.

Nucleation is a statistical phenomenon, so that the time of first nucleation is not always predictable (Toschev *et al.*, 1972; Toschev, 1973). Gibb (1974) observed a time interval of random nucleation of plagioclase. On the other hand, the incubation time of the olivine nucleation is almost fixed and is predictable (Donaldson, 1979). Lofgren (1980) pointed out the importance of the random nature of nucleation to dynamic crystallization studies. However, this randomness has not yet been well understood in geologically important systems.

In the present study, the delay in nucleation of diopside and anorthite was investigated as a function of degree of supercooling, cooling rate, and time. To evaluate the role of the physical state of liquid, effects of initial superheat and of its duration were also investigated. In addition, the effect of heterogeneous nucleation was studied. The present results, both concerning the delay in nucleation and its randomness, are discussed in terms of non-steady state nucleation theory in which probabilistic aspects are taken into account.

Experimental technique

Synthetic glasses of three different compositions were prepared by repeated fusion and grinding of oxide–carbonate mixtures. Chemical compositions of the three starting materials, named Di_{80}, Di_{64} and Di_{50}, are listed in Table 1 together with their liquidus temperatures. They are shown in the phase diagram of the system diopside–anorthite in Figure 1a. The powdered glasses were pressed into pellets (2–4 mm in diameter and 1–2 mm thick) hung on Pt loops made from 0.1 mm wire. Some runs using Di_{80} were carried out using $Pt_{90}Au_{10}$ capsules (5 mm in diameter and 10–15 mm long) in order to examine the effect of the container or the effect of the heterogeneous nucleation. Four charges were hung simultaneously at corners of crossed horizontal ceramic bars (about 15 mm long) at the hot spot of a one-atmosphere vertical furnace under atmospheric conditions. A Pt-Pt_{13}Rh thermocouple calibrated against the melting temperature of gold was placed at the center of the crossed bars to monitor temperature. Horizontal temperature differences at the hot spot were within ±1°C. In order to examine the effect of ΔT and cooling rate, two temperature programs were applied; after the charges were completely melted at temperatures 30–40°C above the liquidus temperatures (*i.e.*, initial superheat, 30–40°C) for 3 hours (*i.e.*, duration of the initial superheat, 3 hours), the charge was either (1) dropped rapidly (approximately 2000°C/hr) to a desired isothermal crystallization temperature 10 to 250°C below the liquidus temperature or (2) cooled at a desired, constant cooling rate of 0.33 to 530°C/hr. The former are called "isothermal crystallization experiments", and the latter "continuous cooling experiments". The four charges in the furnace were quenched into water at different times varying from 1 min to 2 weeks in the isothermal crystallization experiments and at different quench temperatures varying from 1400 to 900°C in the continuous cooling experiments. Temperature programs used in the two types of the experiments are shown in Figure 1b,c. The additional isothermal crystallization experiments using Di_{50} were conducted in order to examine the effects of initial superheat and its duration. The charges in these experiments were melted at various superliquidus temperatures (5–80°C) for 3 hours or melted for various lengths of time from 5 to 760 min at 1420±2°C, and were dropped to a crystallization temperature of 1314±2°C. Equilibrium experiments were also carried out by using glassy or crystalline charges of the starting materials (Table 2).

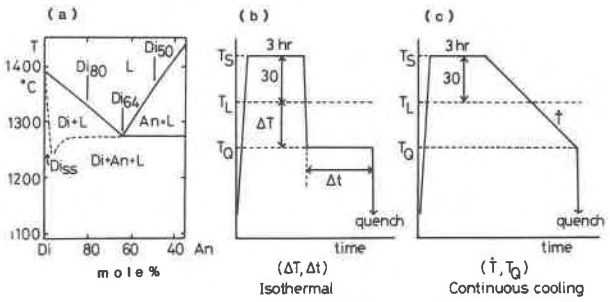

Fig. 1. Schematic illustrations of the experimental conditions. (a) Three different compositions of starting materials (Di_{80}, Di_{64} and Di_{50}) plotted on the phase diagram of the system diopside–anorthite. (b) Temperature–time program used in the isothermal crystallization experiments. (c) Temperature–time program used in the continuous cooling experiments.

Table 1. Chemical compositions (wt%) of starting materials

wt%	Di80	Di64	Di50
SiO_2	52.03	48.92	48.17
Al_2O_3	8.19	14.96	20.58
MgO	13.92	10.60	7.88
CaO	24.58	23.75	22.81
Total	98.71	98.24	99.44
Di(mole%)*	81.1	64.2	49.2
Liquidus phase	Di	Di,An	An
Temperature**	1330°C	1270°C	1360°C

* Diopside contents are determined by MgO/(MgO+Al_2O_3).
** Liquidus Temperatures are determined by the equilibrium experiments.

Run products were mounted with epoxy and were cut into two or more slices to prepare thin sections in order to observe phases under the microscope. The run products were observed carefully under the binocular microscope before cutting in order to minimize the error resulting from cutting in the wrong place.

Results

In the Di_{80} and Di_{64} compositions, diopside always appears first followed by anorthite, whereas anorthite appears first followed by diopside in the Di_{50} composition, except for isothermal crystallization experiments at large ΔT. Forsterite appears in only one charge of Di_{80}

Table 2. Results of equilibrium experiments

	Temperature °C	Duration hr	Starting materials	Products
Di80	1336	15.0	G	gl
	1334	45.0	G	gl
	1332	62.9	G	gl,di
	1330	28.5	G	gl
	1326	43.7	G	gl,di
	1323	167.0	G	gl,di
Di64	1275	161.6	X	gl
	1268	76.0	G	gl
	1268	290.3	X	gl,di,an
	1262	278.9	X	gl,di,an
	1256	214.9	X	gl,di,an
Di50	1372	95.7	G	gl
	1364	99.4	G	gl
	1363	100.0	X	gl
	1360	85.1	X	gl,an?
	1357	85.2	X	gl,an
	1356	108.5	G	gl,an

Starting materials : G = glassy, X = crystalline
Products : gl = glass, di = diopside, an = anorthite

cooled at 1.3°C/hr and quenched at 1116°C. The crystals of all phases sometimes grow from the Pt-wires or the Pt-Au capsule walls.

The appearance of diopside and of anorthite is always delayed under supercooled conditions. Figures 2a, b, 3 and 4 show the delay in the phase appearance in the isothermal crystallization and the continuous cooling experiments using Pt-wire loops. The highest temperature in each figure indicates the liquidus temperature. Each point in the figures shows a phase assemblage at a given crystallization temperature (and thus ΔT) and run duration in the isothermal crystallization experiments, and quench temperature and its run duration in the continuous cooling experiments, respectively.

Isothermal crystallization experiments

In the isothermal crystallization experiments, no crystalline phase appears in the temperature–time region indicated by GL (Figs. 2a, 3a and 4a). In the region indicated by GL±DI, some charges contain diopside and some are still all glass for Di_{80} (Fig. 2a) and Di_{64} (Fig. 3a). In the region indicated by GL±AN, some charges contain anorthite and some are still all glass for Di_{50} (Fig. 4a). In the region indicated by GL+DI (Figs. 2a and 3a) and GL+AN (Fig. 4a), the charges always contain diopside and anorthite, respectively. The region of the random appearance of diopside (GL±DI) is wider than that of anorthite (GL±AN). Despite the randomness, the delay in the phase appearance has a tendency to decrease with increasing ΔT. On further increase in ΔT, the delay in the anorthite appearance increases (Fig. 4a). The curve showing anorthite appearance in the figure is C-shaped, and the minimum delay (nose) of the C-curve is at about 100°C ΔT. Anorthite does not appear from Di_{80} in the temperature range of the experiments (Fig. 2a). It appears from Di_{64} as the second phase with a narrow range of randomness. (Fig. 3a, and double circles with question marks in the figure show the charges in which a small amount of very fine crystals of anorthite seems to be present within arms of diopside dendrites. However it is very difficult to confirm whether or not anorthite is present).

Diopside appears from Di_{50} with a wide range of randomness (Fig. 4a); in the time–temperature range from 10–1000 min and less than 1220°C, some of the charges containing glass + diopside + anorthite are considered to be formed by primary appearance of diopside immediately followed by entry of anorthite. The appearance of

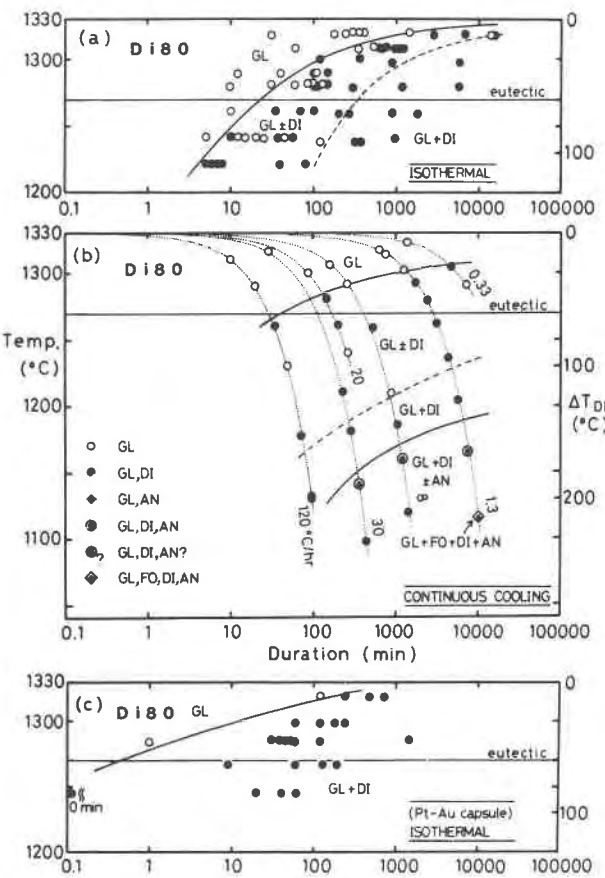

Fig. 2. Experimental results on the delay in nucleation for Di_{80}. Mineral assemblages which appeared in charges are plotted on the crystallization temperature (and thus ΔT) duration diagram in the isothermal crystallization experiments and on quench temperature–run duration diagram in the continuous cooling experiments. Symbols showing the mineral assemblages are given in (b). GL: glass; DI: diopside; AN: anorthite; FO: forsterite. The liquidus of diopside is at about 1330°C, and the diopside–anorthite eutectic is at about 1270°C. (a) Isothermal crystallization experiments with Pt-wire loops. (b) Continuous cooling experiments with Pt-wire loops. The run duration was measured from the time at which temperature passed through the liquidus. Dashed logarithmic curves show constant cooling paths and their rates are also given in °C/hr. (c) Isothermal crystallization experiments with Pt–Au capsules.

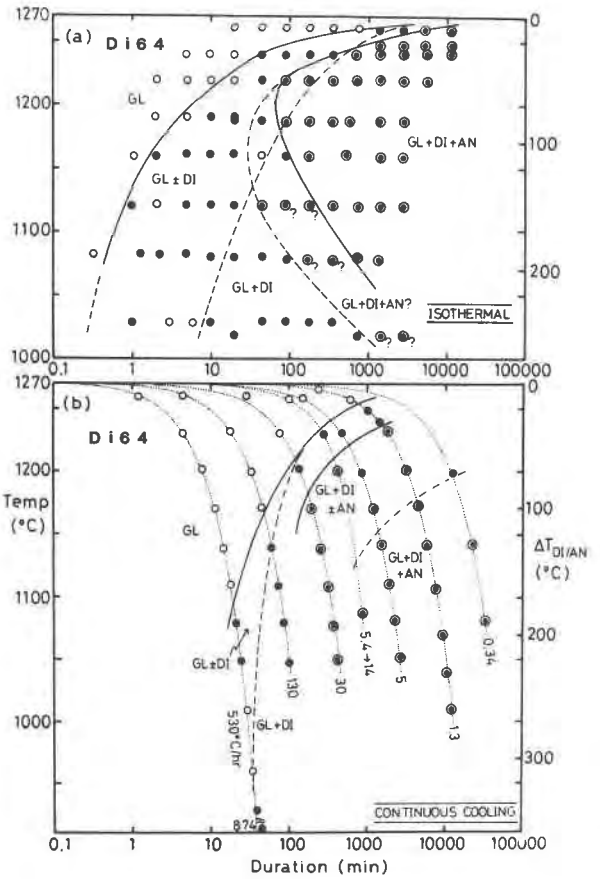

Fig. 3. Experimental results on the delay in nucleation for Di_{64} with Pt-wire loops. Symbols are the same as those in Fig. 2b. The diopside–anorthite eutectic is at about 1270°C. (a) Isothermal crystallization experiments. (b) Continuous cooling experiments.

diopside seems to be random in the regions indicated by GL±DI±AN and GL+AN because the charges containing only glass and glass + anorthite are present in these regions. This reversal of the appearance of phases is not clear from the texture of these charges (spherulitic or dendritic intergrowth of diopside and anorthite) which would appear to show simultaneous nucleation of both phases. As in the appearance of diopside from Di_{80} and Di_{64} and of anorthite from Di_{50}, the delay in the appearance of anorthite from Di_{64} and diopside from Di_{50} decreases with increasing ΔT and the anorthite appearance also has a nose.

Effect of Pt-Au capsule

Figure 2c shows the results of diopside appearance from Di_{80} in the isothermal experiments with the Pt-Au capsules. Diopside appears with a narrower range of temperature of random appearance than in the experiments with the Pt-wire loops (Fig. 2a). The delay in the appearance is also smaller.

Continuous cooling experiments

In the continuous cooling experiments, the phases also appear in a random region (Figs. 2b, 3b and 4b). However, there is no systematic tendency as found in the isothermal crystallization experiments; for example, the range of the random appearance of diopside from Di_{64} (Fig. 3b) and Di_{50} (Fig. 4b) is narrow whereas that of anorthite from Di_{50} (Fig. 4b) is wide. This could be the result of fewer data in the continuous cooling experiments than in the isothermal crystallization experiments. The temperature at which a phase appears decreases with increasing cooling rate. Because the run duration decreases with increasing cooling rate, the phase appearance curves are similar to those in the isothermal crystallization experiments, but they are not identical to each other. The anorthite appearance curve in Di_{64} also has a

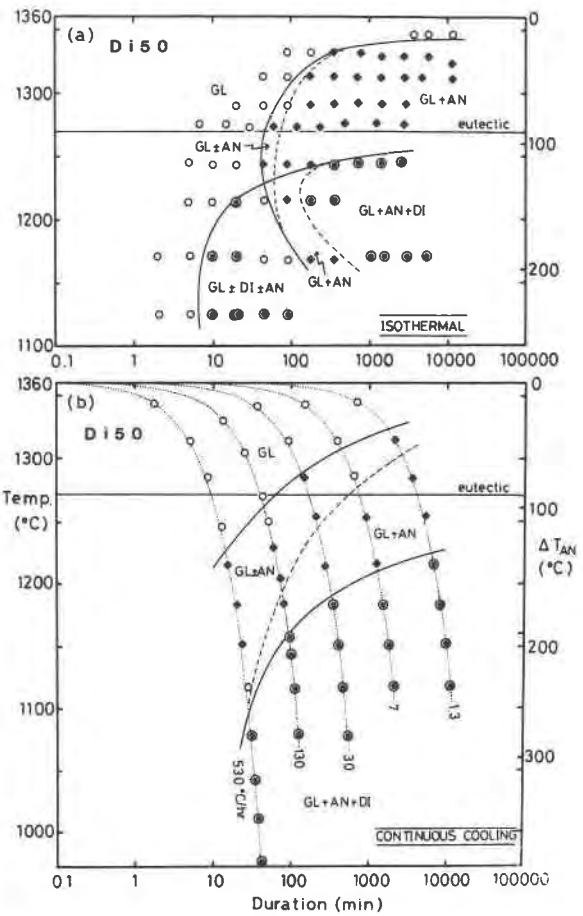

Fig. 4. Experimental results on the delay in nucleation for Di_{50} with Pt-wire loops. Symbols are the same as those in Fig. 2b. The liquidus of anorthite is at about 1360°C. (a) Isothermal crystallization experiments. (b) Continuous cooling experiments.

nose (Fig. 3b); anorthite appears with cooling rates less than 30°C/hr (the lower half of the C-curve is not drawn in the figure because the curve is tangent to the cooling path at the nose). However, the anorthite appearance curve in Di_{50} does not have a nose in the time–temperature range of the experiments (Fig. 4b).

Effects of initial superheating and its duration

Effects of the initial superheat and its duration on anorthite appearance for Di_{50} were examined in the isothermal crystallization experiments. Results are shown in the initial superheat–run duration diagram (Fig. 5a) and the initial heating duration–run duration diagram (Fig. 5b), respectively. Fig. 5a shows that the delay in the anorthite appearance is practically constant at heating temperatures greater than about 1400°C (initial superheats greater than about 40°C), whereas the delay decreases with decreasing heating temperature at less than about 1400°C. On the other hand, Figure 5b shows that the delay is practically constant for heating durations greater than about 45 min, whereas the delay decreases with decreasing the heating duration of less than about 45 min.

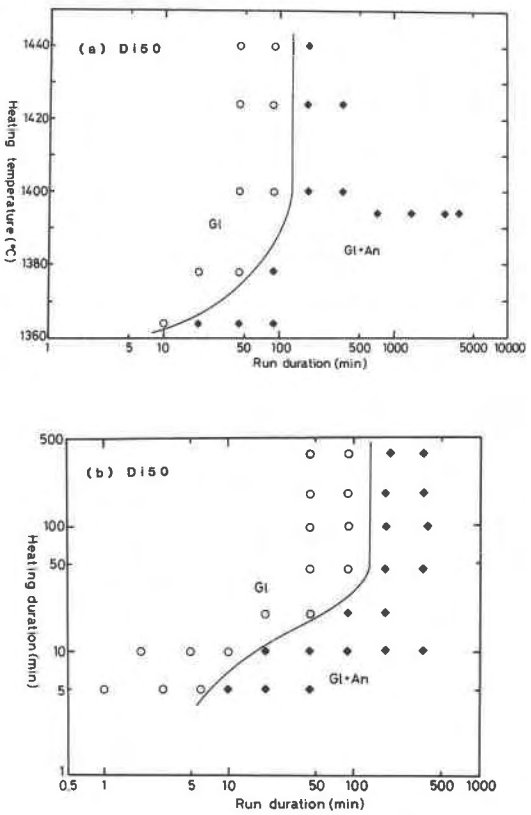

Fig. 5. Effects of the initial superheat and its duration on the delay of the nucleation of anorthite for Di_{50} in the isothermal crystallization experiments with Pt-wire loops. Symbols for mineral assemblages are the same as those in Fig. 2b. The crystallization temperature is 1314±2°C (ΔT = 46±2°C). (a) Effect of the initial superheat. Duration of the initial heating is 3 hours. The anorthite primary liquidus is at about 1360°C. (b) Effect of the duration of the initial superheat. The initial heating temperature is 1400±2°C (the initial superheat is 40±2°C).

Nucleation theory

Donaldson (1979) explained his experimental results in terms of nucleation theory. The theory of nucleation in silicate melts has been also reviewed by Dowty (1980) and Kirkpatrick (1981). However, random nucleation cannot be treated in these theories because they do not take probabilistic aspects of nucleation into consideration. In the present study, the results will be explained in terms of steady-state and transient nucleation and its probabilistic nature as reviewed below.

It is believed that a liquid contains "clusters" of atoms, ions, or molecules, some of which have the structure of the solid which can crystallize from the liquid (*e.g.*, Chalmers, 1964). Because of the surface energy of these embryonic clusters, clusters of the critical size have a chance to survive and to grow to macroscopic sizes only within supercooled or supersaturated systems. In classical nucleation theory a chain reaction, in which a cluster of i-atoms (i-mer) gains an atom to become an (i+1)-mer or loses an atom to become an (i-1)-mer, is considered. By solving steady-state size distribution of the clusters, one can obtain the steady-state nucleation rate, I_0 (*e.g.*, Toschev, 1973).

If a liquid is cooled rapidly to a supercooled condition, the steady-state cluster distribution can not be attained instantaneously. If only monomers are present at the initial moment, the transient nucleation rate, I, can be calculated by solving the transient state cluster distribution as a function of time, t, (Toschev, 1973);

$$I = I_0\left(1 + 2\sum_{s=1}^{\infty}(-1)^s \exp(-s^2t/\tau)\right), \qquad (1)$$

where τ, called induction time or non-steady-state time lag, is a measure of the time necessary for the nucleation rate to reach the steady-state value, I_0, and s is an integer.

Nucleation is a random phenomenon. If the probability of finding m nucleii of super-critical size within a time interval can be described by a Poisson distribution, the probability of discovering the first nucleus (m = 1), P, in a sample with a volume, V, can be derived as a function of time, t (Toschev *et al.*, 1972);

$$P = 1 - \exp\left(-\int_0^t I(t)V dt\right). \qquad (2)$$

Toschev *et al.* (1972) showed that the P-t relations can be estimated from Equations (1) and (2), if values of I_0, τ and V are known. Examples are given in Figure 6 for steady-state and transient nucleation. It is seen from Figure 6 that the range of random nucleation in which

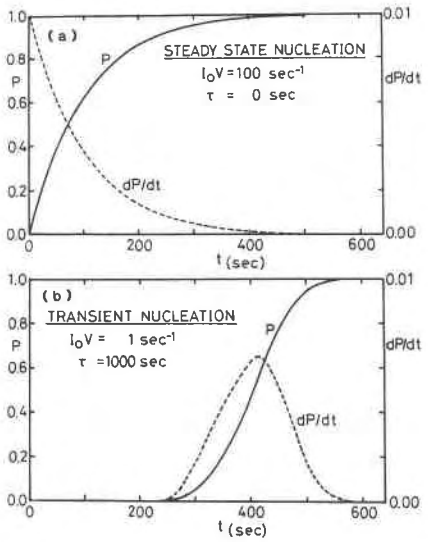

Fig. 6. Examples of calculated nucleation probability, P, as a function of time, t, determined from Eqs. (1) and (2) with a given supercooling. dP/dt is also given as dashed lines. (a) Steady-state nucleation. (b) Transient nulceation.

some samples contain a nucleus and some do not, is wider for steady-state nucleation than for transient nucleation.

If nucleation takes place heterogeneously on a substrate, and the "wetting" between the substrate and the nucleus is good, the steady-state rate of heterogeneous nucleation becomes much greater than that of homogeneous nucleation. It is expected from the expression for the incubation time (Toschev, 1973) that the incubation time is practically unchanged, but becomes small if the wetting becomes extremely good.

Application of the nucleation theory to silicate liquids

The above nucleation theory treats liquids with simple structures. The problem, therefore, is whether the assumption of the reaction between i-mer clusters is still valid for nucleation in silicate liquids. In other words, what is the minimum unit of the cluster? Raman spectroscopic studies suggest that "monomer", "dimer", "chain", "sheet" and "3-dimensional network" species of TO_4 tetrahedra (T = Si, Al, and other small cations) can be distinguished in silicate melts (Mysen *et al.*, 1980). Although these species in the melts are supposed to correspond to silicate mineral-like clusters, many of them are not the same as those in the structures of silicate minerals. Simulation of $MgSiO_3$ melts by molecular dynamics shows that chain-like polymers of SiO_4 tetrahedra do not imply the existence of the same infinite SiO_4 chains as those in pyroxenes (Matsui and Kawamura, 1980). Furthermore the structures of the melts are not static. From this viewpoint, the minimum unit of the cluster may be composed of a TO_4 tetrahedron with appropriate cations and oxygen atoms, and the reaction between clusters in silicate liquids may be regarded as addition/removal of the minimum unit to/from a mineral-like cluster which does not usually correspond to a polymer species. The validity of this assumption will be discussed later based on the experimental results.

Discussion

A delay in phase appearance in the previous experiments can be interpreted in one of two ways; (1) slow growth of new particles and (2) delay in nucleation. The time for the growth of a nucleus to a visible size estimated from the data of the growth rates of diopside and anorthite grown from their own melts (Kirkpatrick *et al.*, 1976) is much less than the incubation time of the phase appearance in the present experiments for a given ΔT (Table 3). This suggests that the delay in the appearance of crystals in the present experiments is due to the delay in nucleation. It should be noted that some nucleation in the experiments is heterogeneous, because the crystals sometimes grow from the Pt-wires or the Pt-Au capsule walls.

Only the nucleation of the primary phases (diopside in Di_{80} and Di_{64}, and anorthite in Di_{50}) will be discussed here because the residual liquid composition has been changed and usually is heterogeneous due to compositional gradients at the time of the nucleation of the second phases (Tsuchiyama, in preparation).

Nucleation randomness in the isothermal crystallization experiments

As shown in Figure 6, it is expected that steady-state nucleation takes place with a wider range of random nucleation than does transient nucleation. If the first nucleus is actually discovered in the time interval between t_0 and t_1, the time width of the random nucleation, W, and the mean incubation time, t*, can be expressed as follows;

$$W = (t_1 - t_0)/(t_1 + t_0) \quad (3)$$

and

$$t^* = (t_1 + t_0)/2. \quad (4)$$

Table 3. Growth rates of diopside and anorthite from their own melts, R, (Kirkpatrick *et al.*, 1976), times for the growth of the nuclei to visible sizes (10 μm), t_{10}, and incubation times as a function of degree of supercooling, ΔT.

	Diopside				Anorthite		
			Incubation time				Incubation time
ΔT	R	t_{10}	Di80	Di64	R	t_{10}	Di50
°C	cm/min	min	min	min	cm/min	min	min
10	0.03	0.03	1500-40000	1000-4500	0.003	0.3	>>10000
20	0.2	0.005	300- 4000	110- 900	0.03	0.03	1500
40	0.4	0.003	65- 900	25- 300	0.08	0.01	200
80	0.7	0.001	10- 200	2.5- 65	0.2	0.005	50-70
160	1	0.001		0.7- 25	0.8	0.001	65

These can be estimated from Equations (1) and (2) by calculating t_0 and t_1, and are shown graphically in the $I_0V - \tau$ diagram (Fig. 7). In this calculation t_0 and t_1 are the times at which the first nucleus is discovered with the probabilities P = 0.03 and P = 0.97. Figure 7 shows that W is a function of only $I_0V\tau$ and increase with decreasing $I_0V\tau$. When $I_0V\tau < 1$, steady-state nucleation takes place, and when $I_0V\tau \gg 1$, transient nucleation takes place. $I_0V\tau$ is a measure of steady-state or transient nucleation. The mean incubation time, t*, is related to $I_0V\tau$ and thus W, $t^* = 1/I_0V$ for $I_0V\tau < 1$ (steady-state nucleation, W ~ 1), and is approximately proportional to τ for $I_0V\tau \gg 1$ (transient nucleation, W ~ 0).

In the isothermal crystallization experiments with Pt-wire loops, the range of random nucleation of diopside is wide (Figs. 2a and 3a) whereas that of anorthite is narrow (Fig. 4a). According to the above model, this indicates that steady-state nucleation takes place for diopside ($I_0V\tau < 1$), whereas transient nucleation takes place for anorthite ($I_0V\tau \gg 1$). The values of W and t* can be roughly estimated from the experimental results; for example at

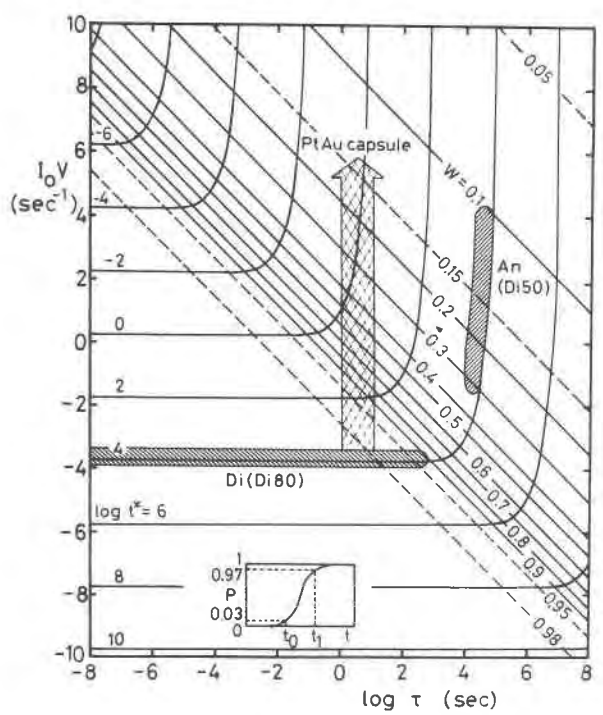

Fig. 7. The measure of the nucleation randomness, $W = (t_1 - t_0)/(t_1 + t_0)$, and the mean incubation time, $t^* = (t_1 + t_0)/2$, shown graphically as a function of I_0V and τ. Discrepancy between the values of t* and $1/I_0V$ when $I_0V\tau < 1$ is due to taking $t_0 = t(P = 0.03)$ and $t_1 = t(P = 0.97)$. The hatched areas indicate the regions of I_0V-τ estimated from the experimental results of diopside nucleation for Di_{80} and anorthite nucleation for Di_{50}, respectively, at $\Delta T = 70°C$. The hatched arrow indicates the effect of heterogeneous nucleation on the wall of Pt–Au capsules.

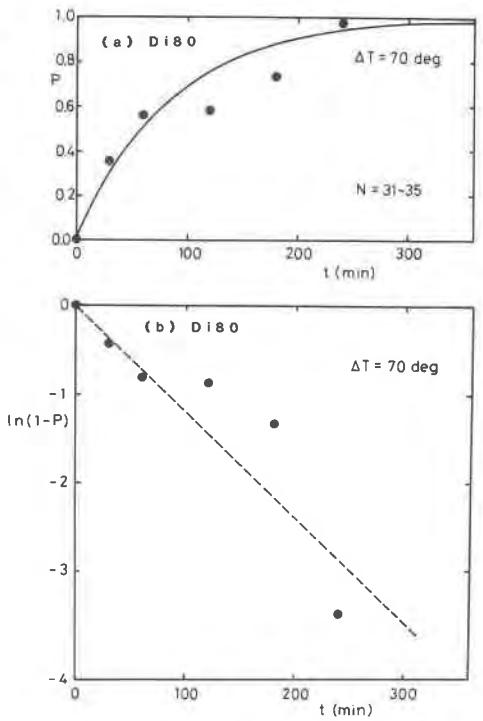

Fig. 8. (a) Probability of finding diopside crystals, P, plotted against run duration, t, in the isothermal crystallization experiments, in which starting gels with the composition similar to Di_{80} are melted at 1360±2°C for 3 hours before dropping to the crystallization temperature ($\Delta T = 70±2°C$). Each P is obtained by 31–35 runs. (b) ln(1-P) plotted against t according to Equation (5).

$\Delta T = 70°C$, W ~ 0.9 and t* ~ 130 min for the nucleation of diopside in Di_{80}, W ~ 0.9 and t* ~ 60 min in Di_{64}, and W ~ 0.2 and t* ~ 80 min for that of anorthite in Di_{50}. Ranges of I_0V and τ estimated from the above values of W and t* are given in Figure 7 (because the data for Di_{64} are plotted close to those for Di_{80}, they are not plotted in this figure for simplicity). The value of $I_0V\tau$ for diopside ($I_0V\tau < 1$) is less than that for anorthite ($I_0V\tau > 10^4$). This result indicates that the total free energy change of nucleation, $\Delta S\Delta T$, for diopside is greater than that for anorthite or the surface tension, σ, for diopside is less than that for anorthite in the experiments, because $I_0V\tau$ is approximately proportional to $\exp(-K\sigma^3/(\Delta S\Delta T)^2)$ according to classical nucleation theory (K is a constant).

To investigate random nucleation in more detail, additional experiments were carried out using gel starting material with Di_{80} composition. All the charges were melted at 1360±2°C for 3 hours and rapidly dropped to the crystallization temperature with $\Delta T = 70±2°C$. 31 to 35 samples were examined for a given run duration to obtain the nucleation probability, P. The results are shown in Figure 8a. It is evident from Figure 6 that steady-state nucleation occurs ($\tau < 1$ min). For steady-state nucleation the nucleation rate is not a function of

time, and Equation (2) is reduced to the following expression:

$$\ln(1 - P) = -I_0 V t. \quad (5)$$

The $\ln(1 - P)$ *vs.* t plot of the results shows a considerable scatter, but the points can be approximately fitted by a straight line given by the steady-state relation, Equation (5) (Fig. 8b). From the slope of the line in Figure 8b, I_0 can be calculated approximately as $1.3 \pm 0.5 \times 10^{-2}$ sec^{-1} cm^{-3} (diameter of the sample is about 0.15 cm). This value is consistent with the value of I_0 ($\sim 1 \times 10^{-2}$ sec^{-1} cm^{-3}, Fig. 7) derived from the mean incubation time at $\Delta T = 70$°C in Figure 2a.

Effect of ΔT

Because steady-state nucleation is considered to take place for diopside, the mean incubation time, t*, for diopside nucleation should be inversely proportional to I_0 ($t^* = 1/I_0 V$). The decrease of the delay in the nucleation of diopside can be explained qualitatively by classical nucleation theory. With increasing ΔT, I_0 increases for relatively small ΔT, so that t* and thus the delay decrease. Because the value of I_0 in Di_{80} can be estimated from the observed value of t* obtained from Figure 2a (Fig. 7), one can estimate the nucleation probability, P, from Equation (5). The estimated P is given in the temperature–time diagram along with the experimental results in Figure 9a. It is clear that only a few charges contain diopside in the region where $P < 10\%$ and all the charges contain diopside in the region where $P > 90\%$.

For anorthite nucleation, on the other hand, the mean incubation time should be proportional to τ because transient nucleation is considered to take place. According to classical nucleation theory, τ decreases and then increases with increasing ΔT. This is also qualitatively consistent with the C-shaped curve of the nucleation of anorthite in Figure 4a. If this explanation is true, the activation energy of a transport process of atoms between liquid and mineral-like clusters can be estimated from the position of the minimum delay (nose) by putting $d\tau/d\Delta T = 0$ and using the values at the nose, $\Delta T = 100$K and $T = 1500$K, and is approximately 50 kcal/mole. This value is comparable to the measured values of the activation energy of self diffusion of Si (70 kcal/mole, Towers and Chipman, 1957) and Al (60 kcal/mole, Henderson *et al.*, 1961) in the system CaO–Al_2O_3–SiO_2. Accordingly, the assumption of the additional/removal of a TO_4 tetrahedron to/from a cluster in silicate melts is reasonable. Uhlmann and Onorato (1979) pointed out that the ratio of the temperature at the nose, T_n, and the liquidus temperature, T_L, is constant for silicates ($T_n/T_L = 0.77$). However, the ratio for anorthite in the present experiments ($T_n/T_L = 0.93$) is significantly higher than 0.77.

Effect of heterogeneous nucleation

The results with the Pt-Au capsules can be explained by the present scheme. Diopside is expected to have a greater chance to nucleate heterogeneously on the capsule walls than it does on the Pt-wires because the contact area with the capsule is much greater than that with the wires, so that I_0 becomes larger. The smaller incubation time and narrower region of random nucleation in the experiments (Fig. 2c) can be explained by the larger I_0 (see arrow in Fig. 7). It has been believed without any evidence that homogeneous nucleation takes place predictably (Donaldson, 1979). On the contrary, however, it becomes evident from the present results that the nucleation becomes more predictable with increasing heterogeneous nature of the nucleation.

Effect of cooling rate

Strictly speaking, for transient nucleation the reaction between i-mer clusters must be solved by taking temperature into account as a function of time if a liquid is continuously cooled. However, because a solution is not available at present, only steady-state nucleation will be considered. In this case the nucleation rate, I, in Equation (2) is determined by only ΔT which is proportional to time, t, if a liquid is cooled with a constant rate, $\dot{T}$. By putting the ΔT-t relation into Equation (2) we obtain

$$P = 1 - \exp\left(-1/\dot{T} \int_0^{\Delta T} I_0(\Delta T)\right) d\Delta T. \quad (6)$$

It is seen from Equation (6) that if a liquid is cooled to a temperature with a given ΔT, P decreases with increasing cooling rate; that is, the nucleation temperature decreases with increasing cooling rate. The results in the continuous cooling experiments are qualitatively consistent with Equation (6). One can estimate P from Equation (6) and $I_0(\Delta T)$ already estimated in the isothermal crystallization experiments for Di_{80}. The estimated P is somewhat different from the experimental results (Fig. 9b). Because of the lack of knowledge about transient nucleation, the probabilistic aspect of the transient nucleation cannot be discussed in more detail.

Effect of superheat and its duration

The incubation time for anorthite nucleation in Di_{50} is unchanged for initial heating temperature greater than about 1400°C (Fig. 5a). According to the equilibrium size distribution of the i-mer clusters in the liquid (Boltzmann distribution, *e.g.*, Toschev, 1973), the clusters are expected to be composed of only monomers ($i = 1$) at temperatures well above the liquidus. The heating duration (3 hours) in the experiments is believed to be sufficient to attain the equilibrium size distribution at 1400°C, as will be discussed later. The decrease of the incubation time with decreasing the heating temperature can be interpreted to indicate that the liquid contains some larger clusters as well as monomers in an equilibrium distribution of the clusters at the lower temperature, or that the heating duration is not sufficient to attain equilibrium distribution at the lower temperature.

When the heating duration is greater than about 45 min

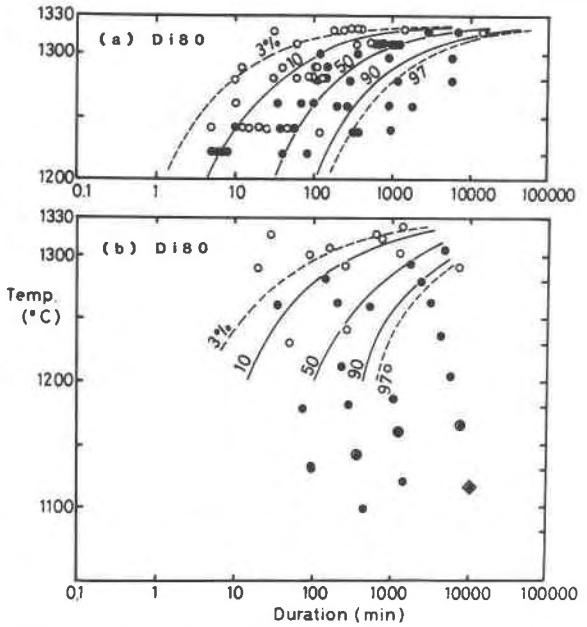

Fig. 9. Comparison between the estimated probability of nucleation of diopside (in %) and the results on the delay of the diopside nucleation for Di_{80}. (a) Isothermal crystallization experiments. The results are the same as those in Fig. 2a. The probability is estimated from Equation (5) and the observed mean incubation time in Fig. 2a. (b) Continuous cooling experiments. The results are the same as those in Fig. 2b. The probability is estimated from Equation (6) and the observed mean incubation time of the isothermal crystallization experiments (Fig. 2a).

at 1400°C, the incubation time of the anorthite nucleation is unchanged (Fig. 5b). This suggests that it takes about 45 min to attain the equilibrium size distribution in the Di_{50} liquid at this temperature. The decrease of the incubation time with decreasing heating duration in Figure 5b can be explained by the original starting glass having some larger clusters. This is also consistent with the observation that very tiny crystals are usually observed in quenched basalt glasses under an electron microscope (Kouchi, pers. comm.). The relaxation time to reach equilibrium would be much smaller than 45 min for the diopside nucleation because steady-state nucleation appears to take place for diopside whereas transient nucleation takes place for anorthite in the isothermal crystallization experiments.

Effect of liquid composition on diopside nucleation

Figure 10 shows the nucleation temperatures plotted on the phase diagram of the diopside–anorthite join. Because of the random nucleation, onset and termination of the first nucleation are shown by solid and open circles, respectively. For compositions with less diopside than Di_{80}, the nucleation temperatures are subparallel to the diopside liquidus. Kirkpatrick *et al.* (1981) carried out continuous cooling experiments with pure diopside composition and found that diopside does not nucleate at least until 1250°C with cooling rates from 10 to 300°C/hr. Their data are also plotted in the same figure. Although it is difficult to compare the two sets of experiments in detail because the glasses may have been prepared differently, it is likely that diopside formation requires less undercooling with increasing anorthite content in the liquid.

Application

TTT and CT diagrams

Figures 2a, c, 3a and 4a and Figures 2b, 3b and 4b are TTT (time–temperature–transformation) and CT (continuous cooling-transformation) diagrams, respectively, which are commonly used to describe the behavior of nucleation. For many metal systems, approximate crystallization behavior can be estimated only from a TTT diagram, because CT curves are shifted to lower temperatures and longer times relative to the TTT curves (Shewmon, 1969). Using this idea, minimum cooling rates for glass formation have been estimated from the TTT diagrams for lunar samples (Uhlmann *et al.*, 1977; Uhlmann and Onorato, 1979). However, in the present experiments the CT curves are not always shifted to lower temperatures and longer times relative to the TTT curves. Donaldson (1979) has also found non-systematic relationships between CT and TTT curves. As a result, estimated cooling rates from the TTT diagrams may have large errors. The randomness of the nucleation, the initial superheat and its duration must be taken into account in a more rigorous treatment.

Cooling rate estimation by dynamic crystallization experiments

There have been many sets of experiments reproducing rock textures or mineral zoning to estimate cooling rate during crystallization (*e.g.*, Donaldson *et al.*, 1975; Grove and Bence, 1977; Grove and Walker, 1977; Walker *et al.*, 1978; Tsuchiyama *et al.*, 1980). If nucleation takes place with a wide range of randomness during cooling as in the present experiments, the textures and the zoning should be different in different runs even at the same cooling rate, because the nucleation temperature (and thus ΔT) is different. What can be estimated from the textures or the zoning pattern, then, is not cooling rate but nucleation temperature (Tsuchiyama, in prep.).

As already discussed, the width of the random nucleation, W, is related to the magnitude of $I_0V\tau$ for the isothermal crystallization (Fig. 7). When crystallization takes place during cooling, the randomness cannot be evaluated for a given sample, as already mentioned. However, from the analogy of the isothermal crystallization the range of random nucleation might be wide if the value of I_0 is relatively small or the relaxation in liquids is relatively rapid. It appears likely from the published data (Walker *et al.*, 1976; Grove and Bence, 1977; Grove,

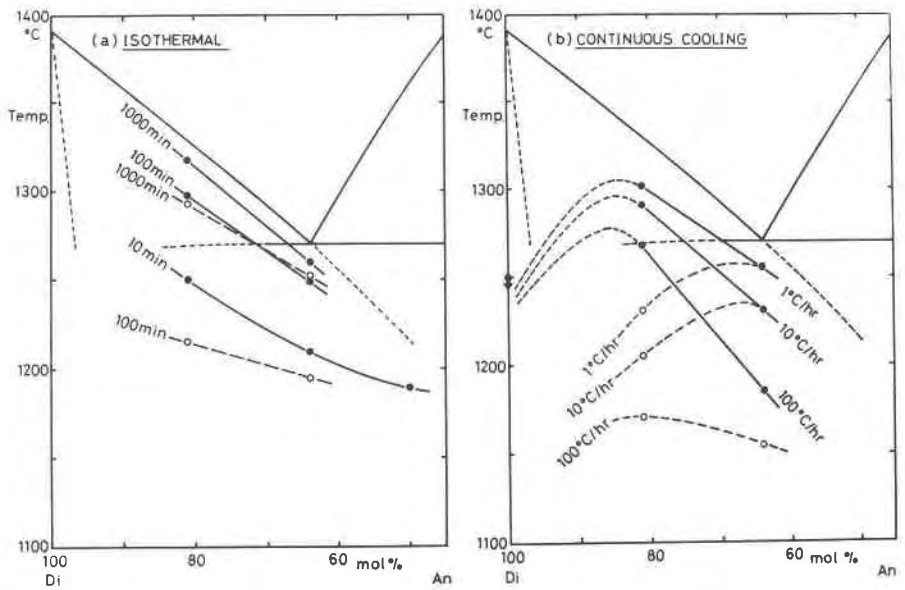

Fig. 10. Onset (solid circles) and termination (open circles) of the first nucleation of diopside obtained from the present experiments with Pt-wire loops (Figs. 2a, 3a and 4a) plotted in the phase diagram of the diopside–anorthite join. (a) Nucleation temperatures corresponding to the three incubation times (1,000, 100 and 10 min). (b) Nucleation temperatures corresponding to the three cooling rates (1, 10 and 100°C/hr). The experimental results that nucleation temperature of diopside in the pure diopside melt cooled with 10–300°C/hr is at least less than 1250°C (Kirkpatrick *et al.*, 1981) are also given.

1978; Donaldson, 1979) that the nucleation usually takes place with a narrow range of randomness. However, these data except for Donaldson (1979) were obtained by experiments using Fe capsules, where heterogeneous nucleation can take place on Fe blebs or the capsule walls (Donaldson *et al.*, 1975). The heterogeneous nucleation leads to an increase in I_0 and thus a decrease in W. The results of Donaldson (1979) might be due to a large I_0 for olivine in his experiments.

Some authors may believe that the range of random nucleation is determined mainly by the mineral itself. For example, Lofgren (1980) pointed out the wide ranges of random nucleation of feldspars. However, the nucleation of anorthite in the present isothermal crystallization experiments shows that the range of random nucleation is narrow (Fig. 4a). It seems that randomness can be determined by both the mineral and the liquid, probably through I_0 and τ.

Effect of superheat and its duration on rock textures

Lofgren (1980) pointed out that textures are strongly affected by whether liquids are cooled from super- or subliquidus conditions, that is, whether crystalline precursors are absent or present. Even when liquids are cooled from super-liquidus temperatures without any visual crystalline precursors, the superheat temperature and its duration may also affect textures and their phase assemblages. It is clear from the anorthite nucleation in the present experiments and from olivine nucleation (Donaldson, 1979) that the nucleation is strongly affected by the initial superheat. In fact, fasciculate texture and porphyritic texture were produced from a eucrite basalt melt with the same cooling rate with small and large initial superheat, respectively (Walker *et al.*, 1978). From a chondrule melt no crystalline phase appears with large initial superheat whereas olivine appears at the same cooling rate with small initial superheat (Tsuchiyama and Nagahara, 1981).

The above results can be explained by the dependence of the equilibrium size distribution of the clusters in liquids on temperature or slow relaxation to equilibrium. However, these effects are not distinguishable if the rate of relaxation is not known. The present experiments (Fig. 5b) show that the time for the relaxation of the Di_{50} liquid is approximately 45 min at 1400°C. If the values of the relaxation time in other silicate liquids are similar in order of magnitude to that of the Di_{50} liquid, durations of initial superheat greater than about 1 hour, which is usually the case in dynamic crystallization experiments, are sufficient to attain equilibrium. In terrestrial and lunar magmas equilibrium is probably attained before eruption. On the other hand, relaxation in liquids is very important for rapid crystallization followed by instantaneous melting such as chondrule crystallization.

Relative ease and reversal of mineral nucleation

In our experiments diopside nucleates before anorthite from the Di_{64} liquid, which is very near the eutectic composition (Fig. 3), and reversal of nucleation of diop-

side and anorthite occurs for Di_{50} at relatively large ΔT (Fig. 4a). Furthermore, the glass + forsterite + diopside + anorthite assemblage produced from Di_{80} in the continuous cooling experiments and its texture (porphyritic texture with forsterite phenocrysts) strongly suggest that forsterite nucleates prior to diopside. There are also many examples of reversal of mineral nucleation (Grove, 1978; Zheng and Yeh, 1979; Naney and Swanson, 1980; Kirkpatrick *et al.*, 1981; Tsuchiyama and Nagahara, 1981). The relative ease and the reversal of mineral nucleation are important for igneous petrology. Modes of minerals in natural igneous rocks have been discussed in terms of the relative ease of mineral nucleation (Wager, 1959; Hawkes, 1967; Naney and Swanson, 1980).

From the previous experimental data mentioned above, the order of the relative ease of mineral nucleation appears to be olivine > pyroxene > feldspar ~ quartz. This order is same as that pointed out by Wager (1959) and Hawkes (1967). However, it should be noted that the relative ease of mineral nucleation cannot be determined only by the mineral itself but must also be related to the liquid. In fact, the mean incubation time of diopside nucleation from Di_{80} (Fig. 2a) is about the same as that of anorthite nucleation from Di_{50} (Fig. 4a), although diopside nucleates more easily than anorthite in Di_{64} (Fig. 3).

Conclusions

(1) Nucleation of diopside and anorthite is delayed under supercooled conditions both in isothermal crystallization and continuous cooling experiments. The delay decreases with increasing degree of supercooling or cooling rate. With further increase in the degree of supercooling or cooling rate the delay in nucleation of anorthite increases. These results can be explained by classical nucleation theory.

(2) For a given degree of supercooling or the same cooling rate, both diopside and anorthite have a time interval in which nucleation may or may not occur (random nucleation).

(3) The temperature–time region of random nucleation of diopside is wider than that of anorthite in the isothermal crystallization experiments. This indicates that steady-state nucleation takes place for diopside whereas transient nucleation takes place for anorthite.

(4) The steady-state nucleation of diopside is verified by obtaining nucleation probabilities as a function of time. From these probabilities the steady-state nucleation rate of diopside is about 1×10^{-2} sec^{-1} cm^{-3} at ΔT = 70°C.

(5) If heterogeneous nucleation is extensive, the delay in nucleation of diopside and region of the random nucleation decreases, probably due to the enhancement of the nucleation rate.

(6) The delay in anorthite nucleation increases and becomes constant with increasing the initial superheat or its duration. These results can be explained by taking into account equilibrium size distribution of crystal embryos with subcritical sizes in the liquid. Relaxation of Di_{50} melt takes about 45 min at 1400°C.

Acknowledgments

I am grateful to Professor I. Kushiro and Y. Nakamura of the University of Tokyo and Dr. M. Kitamura of the Kyoto University for valuable discussion and critical reading of the manuscript.

References

Chalmers, B. (1964) Principles of Solidification. John Wiley & Sons., New York.

Donaldson, C. H. (1979) An experimental investigation of the delay in nucleation of olivine in mafic magmas. Contributions to Mineralogy and Petrology, 69, 21–32.

Donaldson, C. H., Usselman, T. M., Williams, R. J., and Lofgren, G. E. (1975) Experimental modeling of the cooling history of Apollo 12 olivine basalts. Proceedings of the Lunar Science Conference 6th, 843–870.

Dowty, E. (1980) Crystal growth and nucleation theory and the numerical simulation of igneous crystallization. In R.B. Hargraves, Ed., Physics of Magmatic Processes, p. 419–485. Princeton Univ. Press, Princeton.

Fenn, P. M. (1977) The nucleation and growth of alkali feldspars from hydrous melts. Canadian Mineralogist, 15, 135–161.

Gamble, R. P. and Taylor, L.A. (1980) Crystal/liquid partitioning in augite: effect of cooling rate. Earth and Planetary Science Letters, 47, 21–33.

Gibb, F. G. F. (1974) Supercooling and crystallization of plagioclase from a basaltic magma. Mineralogical Magazine, 39, 641–653.

Grove, T. L. (1978) Cooling histories of Luna 24 very low Ti (VLT) ferrobasalts: An experimental study. Proceedings of the Lunar and Planetary Science Conference 9th, 565–584.

Grove, T. L. and Beaty, D. W. (1981) Classification, experimental petrology and possible volcanic histories of the Apollo 11 high-K basalts. Proceedings of the Lunar and Planetary Science Conference 11th, 149–177.

Grove, T. L. and Bence, A. E. (1977) Experimental study of pyroxene-liquid interaction in quartz-normative basalt 15597. Proceedings of the Lunar Science Conference 8th, 1549–1580.

Grove, T. L. and Bence, A. E. (1979) Crystallization kinetics in a multiply saturated basalt magma: An experimental study of Luna 24 ferrobasalt. Proceedings of the Lunar and Planetary Science Conference 10th, 439–478.

Grove, T. L. and Walker, D. (1977) Cooling histories of Apollo 15 quartz normative basalts. Proceedings of the Lunar Science Conference 8th, 1501–1520.

Hawkes, D. D. (1967) Order of abundant crystal nucleation in a natural magma. Geological Magazine, 104, 473–486.

Henderson, J., Yang, L., and Derge, G. (1961) Self-diffusion of aluminum in CaO–SiO_2–Al_2O_3 melts. Transactions of the Metallurgical Society of the AIME, 221, 56–60.

Kirkpatrick, R. J. (1974) Kinetics of crystal growth in the system $CaMgSi_2O_6$–$CaAl_2SiO_6$. American Journal of Science, 274, 215–242.

Kirkpatrick, R. J. (1981) Kinetics of crystallization of igneous rocks. In A.C. Lasaga and R.J. Kirkpatrick, Ed., Kinetics of Geological Processes, vol. 8, p. 321–398. Mineralogical Society of America, Washington.

Kirkpatrick, R. J., Gilpin, R. R., and Hays, J. F. (1976) Kinetics of crystal growth from silicate melts: anorthite and diopside. Journal of Geophysical Research, 81, 5715–5720.

Kirkpatrick, R. J., Kuo, L. C., and Melchior, J. (1981) Crystal growth in incongruently-melting compositions: programmed cooling experiments with diopside. American Mineralogist, 66, 223–241.

Lofgren, G. E. (1974a) An experimental study of plagioclase crystal morphology: isothermal crystallization. American Journal of Science, 274, 243–273.

Lofgren, G. E. (1974b) Temperature induced zoning in synthetic plagioclase feldspar. In W. S. Mackenzie and J. Zussman, Ed., The Feldspars, p. 362–375. Manchester University Press, Manchester.

Lofgren, G. E. (1977) Dynamic crystallization experiments bearing on the origin of textures in impact-generated liquids. Proceedings of the Lunar Science Conference 8th, 2079–2095.

Lofgren, G. E. (1980) Experimental studies on the dynamic crystallization of silicate melts. In R. B. Hargraves, Ed., Physics of Magmatic Processes, p. 487–551. Princeton University Press, Princeton.

Lofgren, G. E. and Gooley, R. (1977) Simultaneous crystallization of feldspar intergrowths from the melt. American Mineralogist, 62, 217–228.

Lofgren, G. E., Donaldson, C. H., Williams, R. J., Mullins, O. Jr., and Usselman, T. M. (1974) Experimentally reproduced textures and mineral chemistry of Apollo 15 quartz normative basalts. Proceedings of the Lunar Science Conference 5th, 549–567.

Matsui, Y. and Kawamura, K. (1980) Instantaneous structure of an $MgSiO_3$ melt simulated by molecular dynamics. Nature, 285, 648–649.

Mysen, B. O., Virgo, D., and Scarfe, C. M. (1980) Relations between the anionic structure and viscosity of silicate melts: a Raman spectroscopic study at 1 atmosphere and at high pressure. American Mineralogist, 65, 690–710.

Naney, M. T. and Swanson, S. E. (1980) The effect of Fe and Mg on crystallization in granitic systems. American Mineralogist, 65, 639–653.

Shewmon, P. G. (1969) Transformations in Metals. McGraw-Hill Inc., New York.

Swanson, S. E. (1977) Relation of nucleation and crystal-growth rate to the development of granitic textures. American Mineralogist, 62, 966–978.

Toschev, S., Milchev, A., and Stoyanov, S. (1972) On some probabilistic aspects of the nucleation process. Journal of Crystal Growth, 13/14, 123–127.

Toschev, S. (1973) Homogeneous nucleation. In P. Hartman, Ed., Crystal Growth: an introduction, p. 1–49. North-Holland Publishing Company, Amsterdam.

Towers, H. and Chipman, J. (1957) Diffusion of calcium and silicon in a lime-alumina silica slag. Transactions of the AIME, 209, 769–773.

Tsuchiyama, A. and Nagahara, H. (1981) Effect of precooling history and cooling rate on the texture of chondrules: a preliminary report. Memoirs of National Institute of Polar Research Special Issue, 20, 175–192.

Tsuchiyama, A., Nagahara, H., and Kushiro, I. (1980) Experimental reproduction of textures of chondrules. Earth and Planetary Science Letters, 48, 155–165.

Uhlmann, D. R. and Onorato, P. I. K. (1979) A simplified model for glass formation. Proceedings of the Lunar and Planetary Science Conference 10th, 375–381.

Uhlmann, D. R., Klein, L. C., and Handwerker, C. A. (1977) Crystallization kinetics, viscous flow, and thermal history of lunar breccia 67975. Proceedings of the Lunar Science Conference 8th, 2067–2078.

Usselman, T. M., Lofgren, G. E., Donaldson, C. H., and Williams, R. J. (1975) Experimentally reproduced textures and mineral chemistries of high-titanium mare basalts. Proceedings of the Lunar Science Conference 6th, 997–1020.

Wager, L. R. (1959) Differing powers of crystal nucleation as a factor producing diversity in layered igneous intrusions. Geological Magazine, 96, 75–80.

Walker, D., Kirkpatrick, R. J., Longhi, J., and Hays, J. F. (1976) Crystallization history of lunar picritic basalt samples 12002: phase equilibria and cooling-rate studies. Geological Society of America Bulletin, 87, 646–656.

Walker, D., Powell, M. A., Lofgren, G. E., and Hays, J. F. (1978) Dynamic crystallization of a eucrite basalt. Proceedings of the Lunar and Planetary Science Conference 9th, 1369–1391.

Zheng, X. and Yeh, D. (1979) On the effect of supercooling crystallization. Scientica Sinica, 22, 453–465.

Manuscript received, May 4, 1982;
accepted for publication, January 10, 1983.